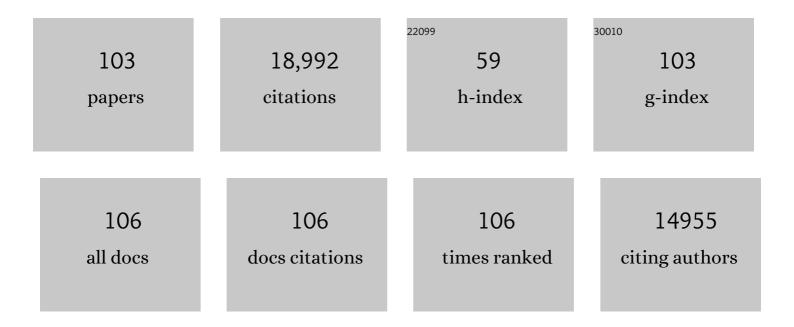
Guofeng Wang

List of Publications by Year in descending order

Source: https://exaly.com/author-pdf/1556634/publications.pdf Version: 2024-02-01



#	Article	IF	CITATIONS
1	Atomistic observation on diffusion-mediated friction between single-asperity contacts. Nature Materials, 2022, 21, 173-180.	13.3	16
2	Atomically dispersed single Ni site catalysts for high-efficiency CO ₂ electroreduction at industrial-level current densities. Energy and Environmental Science, 2022, 15, 2108-2119.	15.6	99
3	Surface oxygenation induced strong interaction between Pd catalyst and functional support for zinc–air batteries. Energy and Environmental Science, 2022, 15, 1573-1584.	15.6	49
4	Passive Oxide Film Growth Observed On the Atomic Scale. Advanced Materials Interfaces, 2022, 9, .	1.9	4
5	Composition-dependent ordering transformations in Pt–Fe nanoalloys. Proceedings of the National Academy of Sciences of the United States of America, 2022, 119, e2117899119.	3.3	10
6	High-entropy nanoparticles: Synthesis-structure-property relationships and data-driven discovery. Science, 2022, 376, eabn3103.	6.0	239
7	Rapid Atomic Ordering Transformation toward Intermetallic Nanoparticles. Nano Letters, 2022, 22, 255-262.	4.5	12
8	Atomically Dispersed Dualâ€Metal Site Catalysts for Enhanced CO ₂ Reduction: Mechanistic Insight into Active Site Structures. Angewandte Chemie - International Edition, 2022, 61, .	7.2	83
9	Atomically Dispersed Dualâ€Metal Site Catalysts for Enhanced CO ₂ Reduction: Mechanistic Insight into Active Site Structures. Angewandte Chemie, 2022, 134, .	1.6	6
10	Atomic-scale friction between single-asperity contacts unveiled through in situ transmission electron microscopy. Nature Nanotechnology, 2022, 17, 737-745.	15.6	9
11	Atomically dispersed iron sites with a nitrogen–carbon coating as highly active and durable oxygen reduction catalysts for fuel cells. Nature Energy, 2022, 7, 652-663.	19.8	258
12	Engineering Atomically Dispersed FeN ₄ Active Sites for CO ₂ Electroreduction. Angewandte Chemie, 2021, 133, 1035-1045.	1.6	39
13	Engineering Atomically Dispersed FeN ₄ Active Sites for CO ₂ Electroreduction. Angewandte Chemie - International Edition, 2021, 60, 1022-1032.	7.2	121
14	Highâ€Entropy Metal Sulfide Nanoparticles Promise Highâ€Performance Oxygen Evolution Reaction. Advanced Energy Materials, 2021, 11, 2002887.	10.2	226
15	Denary oxide nanoparticles as highly stable catalysts for methane combustion. Nature Catalysis, 2021, 4, 62-70.	16.1	153
16	Atomically dispersed single iron sites for promoting Pt and Pt ₃ Co fuel cell catalysts: performance and durability improvements. Energy and Environmental Science, 2021, 14, 4948-4960.	15.6	168
17	Effect of surface steps on chemical ordering in the subsurface of Cu(Au) solid solutions. Physical Review B, 2021, 103, .	1.1	5
18	Dynamically Unveiling Metal–Nitrogen Coordination during Thermal Activation to Design High‣fficient Atomically Dispersed CoN ₄ Active Sites. Angewandte Chemie - International Edition, 2021, 60, 9516-9526.	7.2	119

#	Article	IF	CITATIONS
19	Dynamically Unveiling Metal–Nitrogen Coordination during Thermal Activation to Design Highâ€Efficient Atomically Dispersed CoN ₄ Active Sites. Angewandte Chemie, 2021, 133, 9602-9612.	1.6	21
20	Potential-Dependent Mechanistic Study of Ethanol Electro-oxidation on Palladium. ACS Applied Materials & Interfaces, 2021, 13, 16602-16610.	4.0	20
21	Promoting Atomically Dispersed MnN ₄ Sites <i>via</i> Sulfur Doping for Oxygen Reduction: Unveiling Intrinsic Activity and Degradation in Fuel Cells. ACS Nano, 2021, 15, 6886-6899.	7.3	119
22	On scaling relations of single atom catalysts for electrochemical ammonia synthesis. Applied Surface Science, 2021, 550, 149283.	3.1	15
23	Dualâ€Doping and Synergism toward Highâ€Performance Seawater Electrolysis. Advanced Materials, 2021, 33, e2101425.	11.1	161
24	Enhancing Catalytic Properties of Iron- and Nitrogen-Doped Carbon for Nitrogen Reduction through Structural Distortion: A Density Functional Theory Study. Journal of Physical Chemistry C, 2021, 125, 16004-16012.	1.5	14
25	Atomic Scale Investigation of the CuPc–MAPbX ₃ Interface and the Effect of Non-Stoichiometric Perovskite Films on Interfacial Structures. ACS Nano, 2021, 15, 14813-14821.	7.3	8
26	Coupling between bulk thermal defects and surface segregation dynamics. Physical Review B, 2021, 104,	1.1	3
27	Computational prediction and experimental evaluation of nitrate reduction to ammonia on rhodium. Journal of Catalysis, 2021, 402, 1-9.	3.1	14
28	Atomic Structure Evolution of Pt–Co Binary Catalysts: Single Metal Sites versus Intermetallic Nanocrystals. Advanced Materials, 2021, 33, e2106371.	11.1	62
29	Improving Pd–N–C fuel cell electrocatalysts through fluorination-driven rearrangements of local coordination environment. Nature Energy, 2021, 6, 1144-1153.	19.8	108
30	Atomic‧cale Mechanism of Unidirectional Oxide Growth. Advanced Functional Materials, 2020, 30, 1906504.	7.8	30
31	Boosting CO2 reduction on Fe-N-C with sulfur incorporation: Synergistic electronic and structural engineering. Nano Energy, 2020, 68, 104384.	8.2	106
32	Restoring the Nitrogen Cycle by Electrochemical Reduction of Nitrate: Progress and Prospects. Small Methods, 2020, 4, 2000672.	4.6	225
33	Single Cobalt Sites Dispersed in Hierarchically Porous Nanofiber Networks for Durable and Highâ€Power PGMâ€Free Cathodes in Fuel Cells. Advanced Materials, 2020, 32, e2003577.	11.1	262
34	Acid Stability and Demetalation of PGM-Free ORR Electrocatalyst Structures from Density Functional Theory: A Model for "Single-Atom Catalyst―Dissolution. ACS Catalysis, 2020, 10, 14527-14539.	5.5	105
35	Atomic-scale phase separation induced clustering of solute atoms. Nature Communications, 2020, 11, 3934.	5.8	11
36	Pore-Edge Tailoring of Single-Atom Iron–Nitrogen Sites on Graphene for Enhanced CO ₂ Reduction. ACS Catalysis, 2020, 10, 10803-10811.	5.5	140

#	Article	IF	CITATIONS
37	Atomically Dispersed MnN ₄ Catalysts <i>via</i> Environmentally Benign Aqueous Synthesis for Oxygen Reduction: Mechanistic Understanding of Activity and Stability Improvements. ACS Catalysis, 2020, 10, 10523-10534.	5.5	123
38	Performance enhancement and degradation mechanism identification of a single-atom Co–N–C catalyst for proton exchange membrane fuel cells. Nature Catalysis, 2020, 3, 1044-1054.	16.1	443
39	First-Principles Calculated Structures and Carbon Binding Energies of Σ11 \$\${{left{ {10ar{1}1} ight}} mathord{left/ {vphantom {{left{ {10ar{1}1} ight}} {left{ {10ar{1}ar{1}} ight}}} ight. kern-0pt} {left{ {10ar{1}ar{1}} ight}}\$\$ Tilt Grain Boundaries in Corundum Structured Metal Oxides. Oxidation of Metals. 2020. 94. 37-49.	1.0	0
40	Computationally aided, entropy-driven synthesis of highly efficient and durable multi-elemental alloy catalysts. Science Advances, 2020, 6, eaaz0510.	4.7	158
41	Unlocking the passivation nature of the cathode–air interfacial reactions in lithium ion batteries. Nature Communications, 2020, 11, 3204.	5.8	55
42	Thermal Radiation Synthesis of Ultrafine Platinum Nanoclusters toward Methanol Oxidation. Small Methods, 2020, 4, 2000265.	4.6	16
43	Identification of Efficient Active Sites in Nitrogen-Doped Carbon Nanotubes for Oxygen Reduction Reaction. Journal of Physical Chemistry C, 2020, 124, 8689-8696.	1.5	27
44	Atomically Dispersed Single Ni Site Catalysts for Nitrogen Reduction toward Electrochemical Ammonia Synthesis Using N ₂ and H ₂ O. Small Methods, 2020, 4, 1900821.	4.6	148
45	Atomically Dispersed Iron–Nitrogen Sites on Hierarchically Mesoporous Carbon Nanotube and Graphene Nanoribbon Networks for CO ₂ Reduction. ACS Nano, 2020, 14, 5506-5516.	7.3	125
46	Overcoming immiscibility toward bimetallic catalyst library. Science Advances, 2020, 6, eaaz6844.	4.7	105
47	Lattice doping regulated interfacial reactions in cathode for enhanced cycling stability. Nature Communications, 2019, 10, 3447.	5.8	116
48	3D porous graphitic nanocarbon for enhancing the performance and durability of Pt catalysts: a balance between graphitization and hierarchical porosity. Energy and Environmental Science, 2019, 12, 2830-2841.	15.6	219
49	Thermally Driven Structure and Performance Evolution of Atomically Dispersed FeN ₄ Sites for Oxygen Reduction. Angewandte Chemie, 2019, 131, 19147-19156.	1.6	57
50	Thermally Driven Structure and Performance Evolution of Atomically Dispersed FeN ₄ Sites for Oxygen Reduction. Angewandte Chemie - International Edition, 2019, 58, 18971-18980.	7.2	362
51	Highly efficient decomposition of ammonia using high-entropy alloy catalysts. Nature Communications, 2019, 10, 4011.	5.8	376
52	Surface Defect Dynamics in Organic–Inorganic Hybrid Perovskites: From Mechanism to Interfacial Properties. ACS Nano, 2019, 13, 12127-12136.	7.3	56
53	Efficient CO ₂ Electroreduction by Highly Dense and Active Pyridinic Nitrogen on Holey Carbon Layers with Fluorine Engineering. ACS Catalysis, 2019, 9, 2124-2133.	5.5	97
54	Coordination of Pre-oxidation Time and Temperature for a Better Corrosion Resistance to CO2 at 550°C. Oxidation of Metals, 2019, 91, 657-675.	1.0	4

#	Article	IF	CITATIONS
55	Highly active atomically dispersed CoN ₄ fuel cell cathode catalysts derived from surfactant-assisted MOFs: carbon-shell confinement strategy. Energy and Environmental Science, 2019, 12, 250-260.	15.6	691
56	Mordant inspired wet-spinning of graphene fibers for high performance flexible supercapacitors. Journal of Materials Chemistry A, 2019, 7, 6869-6876.	5.2	47
57	Promoting electrocatalytic CO2 reduction on nitrogen-doped carbon with sulfur addition. Applied Catalysis B: Environmental, 2019, 252, 240-249.	10.8	139
58	Atomic-level active sites of efficient imidazolate framework-derived nickel catalysts for CO ₂ reduction. Journal of Materials Chemistry A, 2019, 7, 26231-26237.	5.2	72
59	Comparison of Microstructural Evolution of Oxides Formed on F91 Martensitic Steel Upon Breakaway Oxidation at 700°C in Air and CO2. Oxidation of Metals, 2019, 91, 463-482.	1.0	1
60	Mn- and N- doped carbon as promising catalysts for oxygen reduction reaction: Theoretical prediction and experimental validation. Applied Catalysis B: Environmental, 2019, 243, 195-203.	10.8	170
61	Atomic-Scale Mechanism of Unidirectional Oxide Growth. Advanced Functional Materials, 2019, 30, .	7.8	2
62	Unveiling Active Sites of CO ₂ Reduction on Nitrogen-Coordinated and Atomically Dispersed Iron and Cobalt Catalysts. ACS Catalysis, 2018, 8, 3116-3122.	5.5	405
63	Metal-organic framework-derived nitrogen-doped highly disordered carbon for electrochemical ammonia synthesis using N2 and H2O in alkaline electrolytes. Nano Energy, 2018, 48, 217-226.	8.2	406
64	Dislocation nucleation facilitated by atomicÂsegregation. Nature Materials, 2018, 17, 56-63.	13.3	99
65	Core–Shell Nanostructured Cobalt–Platinum Electrocatalysts with Enhanced Durability. ACS Catalysis, 2018, 8, 35-42.	5.5	72
66	Solid–Liquid Interfacial Reaction Trigged Propagation of Phase Transition from Surface into Bulk Lattice of Ni-Rich Layered Cathode. Chemistry of Materials, 2018, 30, 7016-7026.	3.2	80
67	Atomically dispersed manganese catalysts for oxygen reduction in proton-exchange membrane fuel cells. Nature Catalysis, 2018, 1, 935-945.	16.1	1,075
68	Revealing Cycling Rate-Dependent Structure Evolution in Ni-Rich Layered Cathode Materials. ACS Energy Letters, 2018, 3, 2433-2440.	8.8	92
69	Segregation induced order-disorder transition in Cu(Au) surface alloys. Acta Materialia, 2018, 154, 220-227.	3.8	11
70	In Situ "Chainmail Catalyst―Assembly in Lowâ€Tortuosity, Hierarchical Carbon Frameworks for Efficient and Stable Hydrogen Generation. Advanced Energy Materials, 2018, 8, 1801289.	10.2	79
71	Observation of Solid-Liquid Interfacial Reactions Controlled Bulk Phase Transition of Ni-rich Layered Cathode. Microscopy and Microanalysis, 2018, 24, 1522-1523.	0.2	1
72	Quantifying solvation energies at solid/liquid interfaces using continuum solvation methods. Molecular Simulation, 2017, 43, 420-427.	0.9	64

#	Article	IF	CITATIONS
73	Role of Local Carbon Structure Surrounding FeN ₄ Sites in Boosting the Catalytic Activity for Oxygen Reduction. Journal of Physical Chemistry C, 2017, 121, 11319-11324.	1.5	150
74	Atomic interpretation of high activity on transition metal and nitrogen-doped carbon nanofibers for catalyzing oxygen reduction. Journal of Materials Chemistry A, 2017, 5, 3336-3345.	5.2	88
75	Charged vacancy diffusion in chromium oxide crystal: DFT and DFT+U predictions. Journal of Applied Physics, 2016, 120, 215101.	1.1	25
76	Bivalence Mn5O8 with hydroxylated interphase for high-voltage aqueous sodium-ion storage. Nature Communications, 2016, 7, 13370.	5.8	109
77	Electrochemical and Computational Study of Oxygen Reduction Reaction on Nonprecious Transition Metal/Nitrogen Doped Carbon Nanofibers in Acid Medium. Journal of Physical Chemistry C, 2016, 120, 1586-1596.	1.5	148
78	Examination of Solid-Solution Phase Formation Rules for High Entropy Alloys from Atomistic Monte Carlo Simulations. Jom, 2015, 67, 2364-2374.	0.9	23
79	Surface faceting and elemental diffusion behaviour at atomic scale for alloy nanoparticles during in situ annealing. Nature Communications, 2015, 6, 8925.	5.8	159
80	Beneficial compressive strain for oxygen reduction reaction on Pt (111) surface. Journal of Chemical Physics, 2014, 141, 124713.	1.2	66
81	Reaction Pathway for Oxygen Reduction on FeN ₄ Embedded Graphene. Journal of Physical Chemistry Letters, 2014, 5, 452-456.	2.1	307
82	Charge Density Determination for Al-rich Composition L1o-ordered gamma-TiAl by Convergent Beam Electron Diffraction. Microscopy and Microanalysis, 2014, 20, 1492-1493.	0.2	0
83	A density functional theory study of oxygen reduction reaction on Me–N4 (Me = Fe, Co, or Ni) clusters between graphitic pores. Journal of Materials Chemistry A, 2013, 1, 10790.	5.2	253
84	Comparison of Reaction Energetics for Oxygen Reduction Reactions on Pt(100), Pt(111), Pt/Ni(100), and Pt/Ni(111) Surfaces: A First-Principles Study. Journal of Physical Chemistry C, 2013, 117, 6284-6292.	1.5	171
85	Density functional calculation of activation energies for lattice and grain boundary diffusion in alumina. Physical Review B, 2013, 87, .	1.1	28
86	Influence of surface segregation on magnetic properties of FePt nanoparticles. Applied Physics Letters, 2013, 103, 132405.	1.5	8
87	Correlation between oxygen adsorption energy and electronic structure of transition metal macrocyclic complexes. Journal of Chemical Physics, 2013, 139, 204306.	1.2	47
88	First-principles transition state study of oxygen reduction reaction on Pt (111) surface modified by subsurface transition metals. Materials Research Society Symposia Proceedings, 2012, 1384, 1.	0.1	1
89	Molecular and Electronic Structures of Transition-Metal Macrocyclic Complexes as Related to Catalyzing Oxygen Reduction Reactions: A Density Functional Theory Study. Journal of Physical Chemistry C, 2012, 116, 16038-16046.	1.5	92
90	High precision electronic charge density determination for L1 ₀ -ordered γ-TiAl by quantitative convergent beam electron diffraction. Philosophical Magazine, 2012, 92, 4408-4424.	0.7	3

#	Article	IF	CITATIONS
91	Influence of Surface Segregation on the Mechanical Property of Metallic Alloy Nanowires. Materials Research Society Symposia Proceedings, 2012, 1424, 127.	0.1	0
92	Design and Synthesis of Bimetallic Electrocatalyst with Multilayered Pt-Skin Surfaces. Journal of the American Chemical Society, 2011, 133, 14396-14403.	6.6	541
93	Synthesis of Homogeneous Pt-Bimetallic Nanoparticles as Highly Efficient Electrocatalysts. ACS Catalysis, 2011, 1, 1355-1359.	5.5	124
94	A first principles study of oxygen reduction reaction on a Pt(111) surface modified by a subsurface transition metal M (M = Ni, Co, or Fe). Physical Chemistry Chemical Physics, 2011, 13, 20178.	1.3	236
95	Modelling the Molecular Transportation of Subcutaneously Injected Salubrinal. Biomedical Engineering and Computational Biology, 2011, 3, BECB.S7050.	0.8	1
96	Correlation Between Surface Chemistry and Electrocatalytic Properties of Monodisperse Pt _{<i>x</i>} Ni _{lâ€<i>x</i>} Nanoparticles. Advanced Functional Materials, 2011, 21, 147-152.	7.8	218
97	In Situ Observation of Small-Scale Deformation in a Lead-Free Solder Alloy. Journal of Electronic Materials, 2009, 38, 400-409.	1.0	20
98	Nanoindentation for measuring individual phase mechanical properties of lead free solder alloy. Journal of Materials Science: Materials in Electronics, 2008, 19, 514-521.	1.1	47
99	Density functional theory study of the adsorption of oxygen molecule on iron phthalocyanine and cobalt phthalocyanine. Molecular Simulation, 2008, 34, 1051-1056.	0.9	70
100	Predicting Young's modulus of nanowires from first-principles calculations on their surface and bulk materials. Journal of Applied Physics, 2008, 104, .	1.1	60
101	Trends in electrocatalysis on extended and nanoscale Pt-bimetallic alloy surfaces. Nature Materials, 2007, 6, 241-247.	13.3	2,902
102	Improved Oxygen Reduction Activity on Pt3Ni(111) via Increased Surface Site Availability. Science, 2007, 315, 493-497.	6.0	3,924
103	Monte Carlo simulations of segregation in Pt-Ni catalyst nanoparticles. Journal of Chemical Physics, 2005, 122, 024706.	1.2	116